Full-Resolution GPR Imaging Applied to Utility Surveying: Insights from Multi-Polarization Data Obtained over a Test Pit

Roger Roberts, David Cist, and Andreas Kathage
GSSI
12 Industrial Way, Salem, NH, 03079, USA
roger@geophysical.com, david_c@geophysical.com, kathagea@geophysical.com

***Abstract*—Full-resolution ground penetrating radar (GPR) imaging requires dense data collection to prevent aliasing during 3D migration. The resulting images of the subsurface are much easier to interpret than 3D images typically obtained from conventional 3D surveys. An investigation has been undertaken to examine potential benefits of full-resolution GPR for utility surveying. An existing test pit with dimensions 12.1 x 12.1 m located at GSSI and containing buried utilities in three different host media was used for the study. Full-resolution GPR (0.05 m inline and cross-line spacing) was obtained at two orthogonal polarizations over the test pit using a 400 MHz center-frequency antenna. The data were processed using two orthogonal 2-D migrations instead of a true 3D migration. Nevertheless, all of the linear targets were successfully imaged from both polarization data. The reason for this is that the amplitude difference of the target reflections between polarizations was typically less than 6 dB and the noise floor was much lower than all the target reflections. In contrast, many of the targets parallel to the data collection direction were not detected when the data were decimated to 0.3m profile line spacing. The full-resolution data also provided a level of detail that potentially could be useful for host media characterization and utility condition monitoring via comparison of time-lapsed datasets.**

***Index Terms*— 2.5D Migration, Full-Resolution GPR, Ground Penetrating Radar, Multi-Polarization, Utility Condition Monitoring, Utility Detection.**

I. Introduction

"Full-resolution" ground penetrating radar (GPR) imaging requires dense data collection to prevent aliasing during 3D migration. Since the resulting images of the subsurface reveal contiguous information in every direction, they are easier to interpret than 3D images typically obtained from conventional 3D surveys. Full-resolution, may be defined as collecting data dense enough so that the size of a voxel (smallest cubical volume element) is smaller than the Nyquist spatial sampling interval at the steepest diffraction in the data [1]. For utility surveys this usually means the angles of the hyperbola tails from pipes. The voxel size, therefore depends on many factors: velocity, depth and noise. Previous full-resolution GPR data have obtained clear images of fractures in limestone [1], stratigraphy in beach sand [2], tree roots [3], and building foundations [3]. This paper presents utility data as confirmation of the power of this method.

There are usually three reasons this technique is not used all the time. First, the data collection part is labor intensive. Since scan density is easy to achieve along a profile line, but laborious from profile to profile. Most surveys suffer from poor lateral resolution, And since profiles must be collected 6-12 times denser than typical 3D GPR surveys, it takes 6 to 12 times longer. Second, the data must be obtained with much greater accuracy than is commonly acceptable for 3D GPR surveys. Scans from neighboring profiles must line up. A comparison of two datasets obtained with a laser positioning system and the traditional odometer wheel methodology in [3] revealed that the random shifting of scans triggered by the odometer wheel substantially impact the resulting 3D image. The data were obtained on grass-covered ground, so it is likely that some wheel slippage and/or topographic variations contributed to the scan shifting. The final limitation of high-resolution GPR imaging is the time required for a full 3D migration which typically requires high-speed parallel CPUs and expensive seismic data processing packages. Consequently, the methodology is currently not commonly used.

However, in GPR technological advances continually break down traditional barriers impeding progress. And so it is anticipated that eventually the benefits of full-resolution GPR imaging for many investigations will outweigh the costs. This investigation was undertaken anticipating the more frequent application of full-resolution GPR imaging to utility surveying.

An existing test pit with dimensions 12.1 x 12.1 m located at GSSI and containing buried utilities in three different host media provided the perfect setting for the study. Fig. 1 shows the test pit configuration.

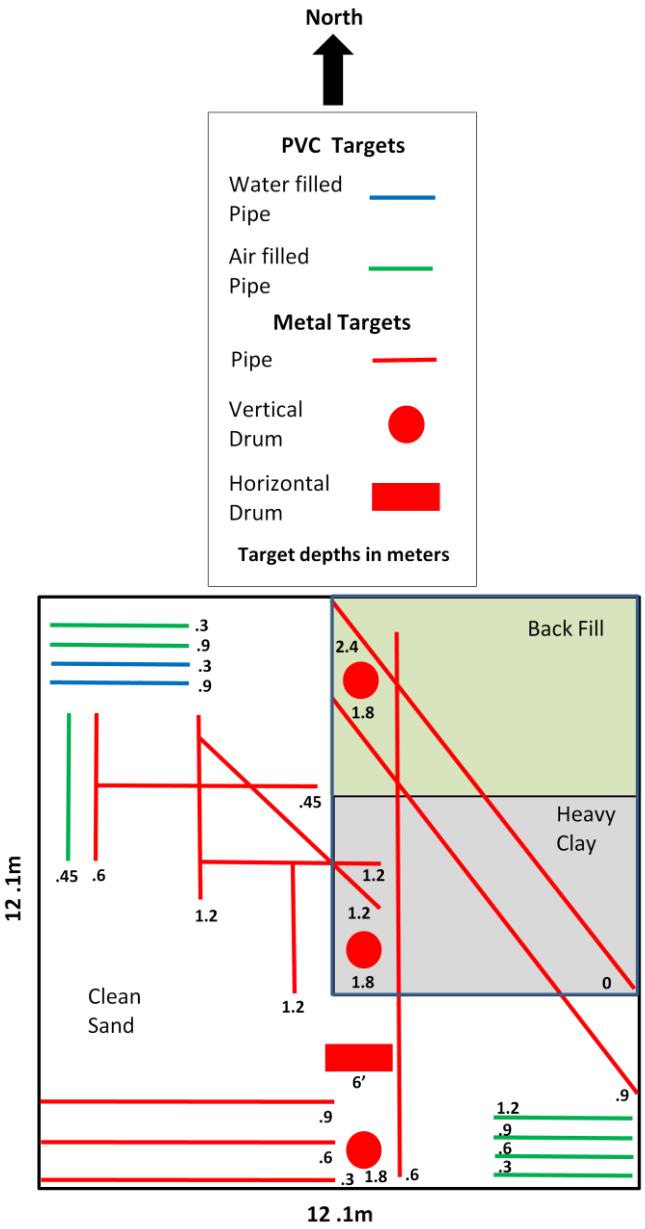

Fig. 1. Test pit located at GSSI used for the investigation. Drawing includes all linear targets buried at depths less than 1.5m. Depths are design depths. Actual depths may differ.

II. DATA COLLECTION

Full-resolution GPR was collected at two orthogonal polarizations over the test pit using a 400 MHz center-frequency antenna. The data were obtained at an inline scan spacing of 0.0125m (decimated to 0.05m in post-processing). The cross- line spacing was 0.05m to meet the minimum sampling requirements for high-resolution imaging [1]. This minimum must be less than ¼ the wavelength of the highest antenna frequency and noise measured. In our case a center-frequency 400 MHz antenna (650MHz high end) in a dielectric of 16 produces a center wavelength of 0.6m. One fourth of the minimum wavelength (0.4m) is 0.1m. A horizontal spacing of half the minimum requirement was chosen to account for any aliasing that might occur due to noise. A total of 241 profile lines were obtained in the East-West direction for each dataset

The required data collection accuracy was achieved using a standard odometer attached to a wheel rim that was constrained by a channel formed by strips of 0.025x0.075 m wood screwed into two connected 7.6m I-Joists. The data collection setup is shown in Fig. 2.

Fig. 2. Data collection over the test pit.

The data collection crew typically consisted of two individuals. One individual would move the data collection cart following the groove by walking backward. The other individual would move the I-Joist 0.05m after each line of data. Each profile took about 40 seconds to collect, but the theoretical 2.6 hours actually required about 4 for each survey. Since there was no discernable odometer wheel slippage, the only measureable inline offsets were associated with slight and occasional variations in start position. The cross-line accuracy was most affected by the flexing of the I-Joist. Between profile lines, the endpoints of the two connected I-joists were accurately positioned. The maximum amount of flexing at the center of the I-joist was estimated to be less than 0.025m.

A full dataset was obtained on August 25, 2008 with the antenna polarization perpendicular to the data collection direction. A second dataset was obtained 11 days later with the antenna polarization parallel to the data collection direction. No rainfall was recorded at two weather stations located within 10 km of GSSI during the 11 day interval.

III. DATA PROCESSING

The data processing steps consisted of (1) resampling the profile line data so as to produce an equi-dimensional 0.05x0.05 m grid interval, (2) application of a time-zero correction; and (3) a simplified constant velocity 2.5D Kirchhoff migration [4]. The Kirchhoff migration was applied first along the profile line direction, then in the orthogonal

direction. The 2.5D migration was implemented for two reasons: (1) it was fast and easy to implement, and (2) most of the targets were horizontal, linear, pipes oriented parallel or perpendicular to the migration direction. Although for this scenario, the 2.5D migration adequately focused the scattered energy from the targets, it is really only proper to use it for constant-velocity media[5].

IV. Data Imaging

The processed data did not require interpolation prior to displaying in 3D. This is important because interpolation is commonly done for conventional 3D surveys due to the data density disparity between the inline and cross-line directions.

The gridded data were viewed in RADAN™ as depth slices of varying thickness. Prior to display, the average amplitude of each depth slice was subtracted.

A full-resolution 0.9m thick depth slice centered at a calculated 0.69m depth containing data obtained with the polarization perpendicular to the profile line direction is shown in Fig. 3. All of the PVC and metal pipes buried at depths less than 1.5m are clearly resolved in the data. A strong reflection in the right central portion of the test pit is associated with the reflection from the top of the clay.

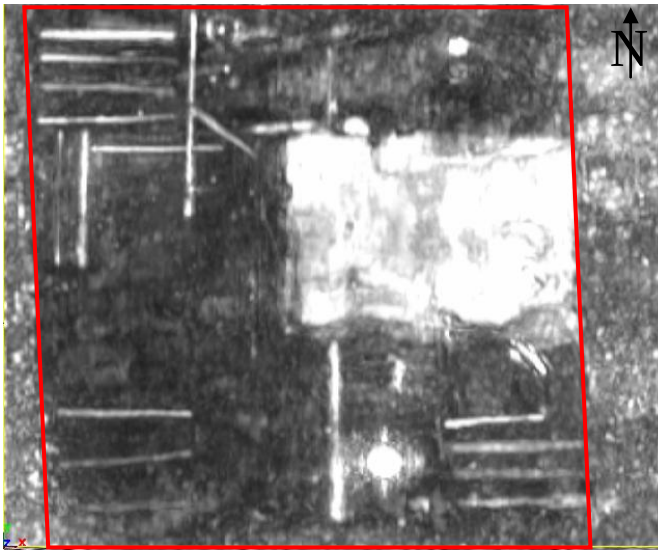

Fig. 3. Full-resolution depth slice of perpendicular polarization data 0.9m thick centered at calculated 0.69m depth. The pit outline is indicated by the red lines.

The same dataset used in Fig. 3, but decimated to 0.3m profile line spacing is shown in Fig. 4. It is clear that all of the pipes perpendicular to the profile line direction are detected using the 0.3m spacing. However, almost all of the pipes parallel to the profile line direction are not detectable in Fig. 4. This is why a 2-D grid of data containing profile lines in orthogonal directions is sometimes implemented to locate utilities.

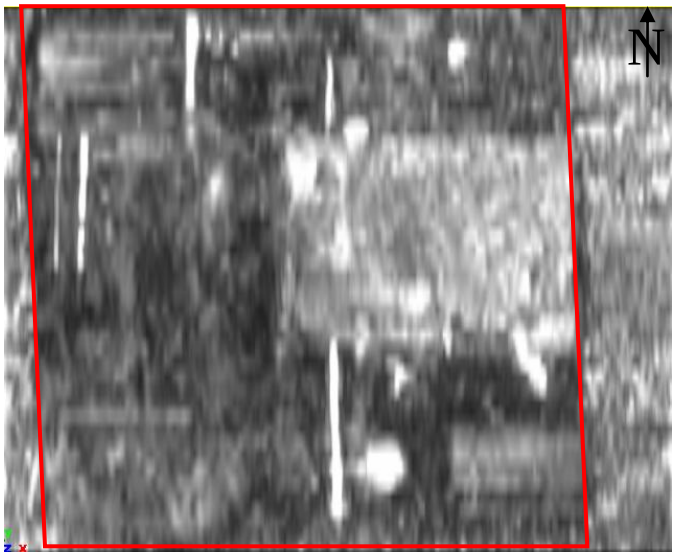

Fig. 4. Typical resolution depth slice of perpendicular polarization data 0.9 m thick centered at calculated 0.69m depth with a (x,y) grid interval of (0.05, 0.30) m . The pit outline is indicated by the red lines.

The corresponding full-resolution depth slice from the data obtained with the polarization parallel to the profile line direction is shown in Fig. 5. Fig. 3 provides a clearer image of the PVC pipes because the polarization direction is perpendicular to the axis of the PVC pipes oriented parallel to the profile line direction.

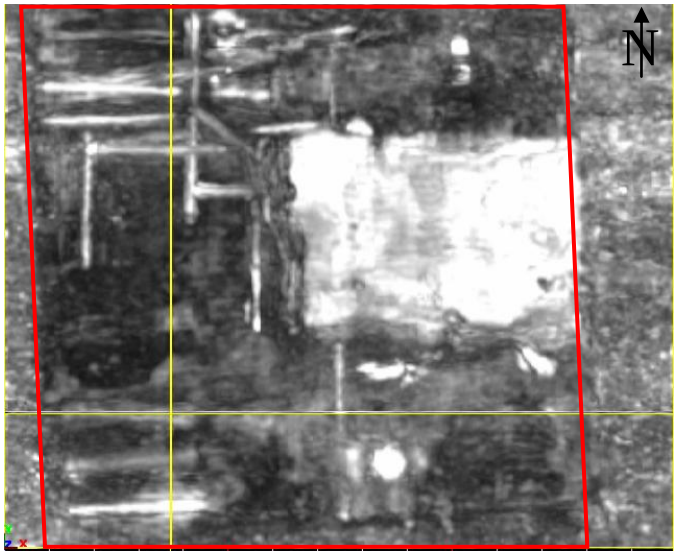

Fig. 5. Full-resolution depth slice of parallel polarization data 0.9m thick centered at calculated 0.69m depth. The pit outline is indicated by the red lines.

Thick depth slices, which are typically obtained by plotting the amplitude of the brightest reflector over the specified depth range at each scan location, are useful for displaying multiple targets at different depths. Unfortunately, this method with thick slices runs the risk of having noise which may overwhelm weaker target reflections, as occurred with the missing 4 PVC pipe reflections in the south-east corner of the test pit in Figure 5. For this reason, it is particularly

important to analyze thin depth slices for the presence of targets. Fig. 6 contains a 0.01 m thick depth slice at parallel polarization data at a calculated depth of 0.97 m. The deepest PVC pipe design depth was at 1.2m. As the slices become thinner, the pipes appear to split open in a "V" shape. This illusion is due either to the dipping nature of the pipe as it is sliced horizontally or a gradual change in medium propagation velocity over the length of the pipe. Slight errors in migration will make the lower ends of the pipe appear broader. A good multi-velocity 3-D migration would correct for some of this error. The required velocity map can be partially assembled using the velocities calculated along the pipes. To do this accurately, a dense target field would be needed.

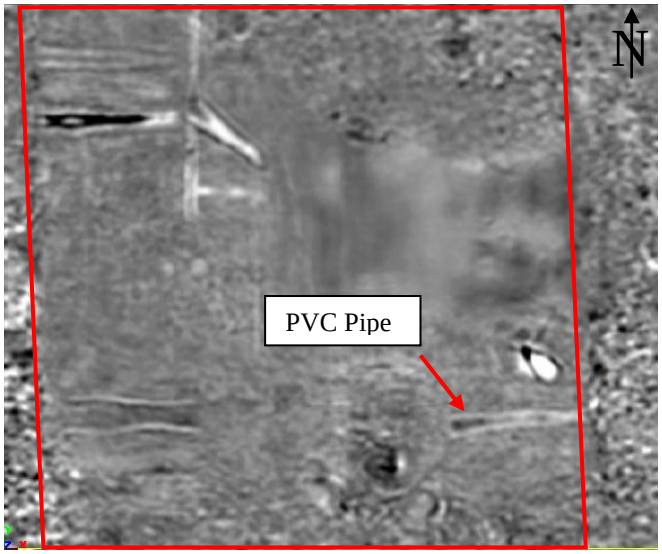

Fig. 6. Full-resolution depth slice of parallel polarization data 0.01m thick centered at calculated 0.97m depth. The pit outline is indicated by the red lines. A PVC pipe reflection is indicated by the arrow.

In Fig. 7 a 0.01 m thick slice of perpendicular polarization data at a calculated depth of 0.57 m is shown. The level of detail in Fig. 7 is impressive. The change in image texture between the native soil and the pit fill material that is demarcated by the red line is clear. The mottled texture outside the pit is generated by scattering from rocks in the native soil. A cross-section of the native soil is shown in Fig. 8. Some layering can be seen as well as numerous 0.05-0.07m diameter rocks scattered throughout the cross-section. One rock near the right side of the figure and indicated by the red circle is 0.10-0.15m in length.

Fig. 7. Full-resolution depth slice of perpendicular polarization data 0.01 m thick centered at calculated 0.56 m depth. The pit outline is indicated by the red lines.

Fig. 8. Cross-section of native soil surrounding the test pit. Note 0.10-0.15m diameter rock (in yellow circle) about 0.3m in depth on right side of picture.

Compare the perpendicularly polarized 0.01m thick depth slice in Fig. 7 with one created using a more typical 0.3x0.05m grid interval in Fig. 9. The pit outline is blurred and the fine details of the scattering from the large aggregate outside the pit are lost.

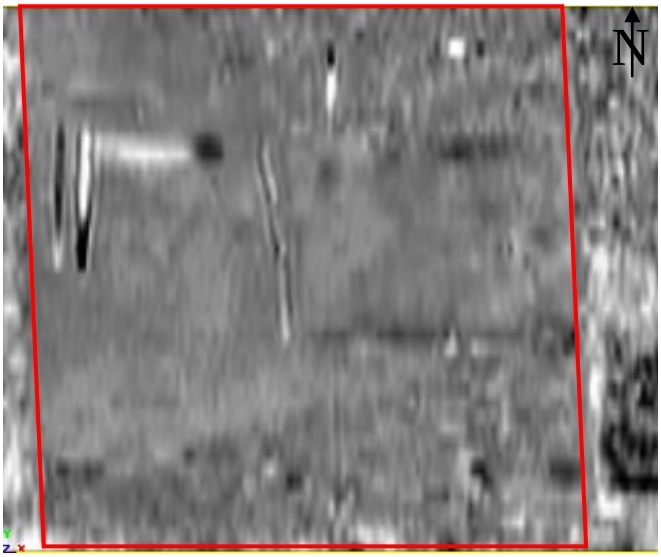

Fig. 9. Typical resolution depth slice of perpendicular polarization data 0.01 m thick centered at calculated 0.56 m depth with a (x,y) grid interval of (0.05, 0.30) m . The pit outline is indicated by the red lines.

A 0.01 m thick depth slice at 0.54 m depth obtained from parallel polarized data at a 0.05x0.05 m grid interval is shown in Figure 10. The slight difference in depth of the slices was necessary to match the scattering pattern in the yellow box with corresponding scattering pattern Fig. 7. (particularly the large dark spots opposite the orange circle).

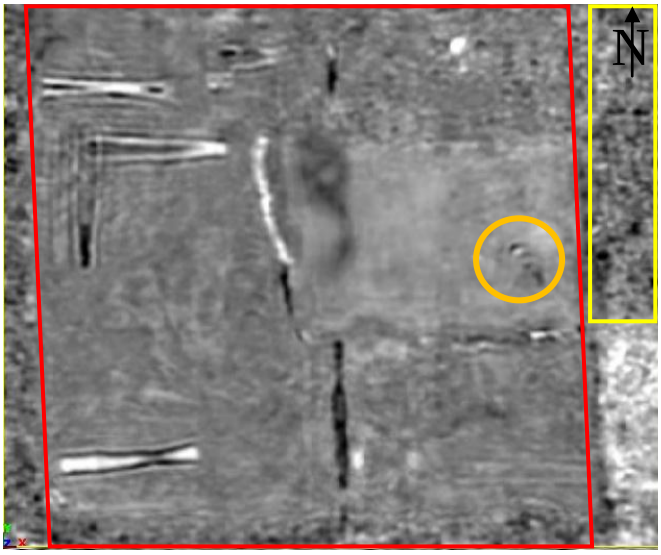

Fig. 10. Full-resolution depth slice of parallel polarization data 0.01m thick centered at calculated 0.54 m depth. The pit outline is indicated by the red lines.

It is also observed from close comparison of Fig. 7 and Fig. 10 that the gray-scale gradations within the clay fill area are nearly identical despite the fact that the data were obtained with different polarizations. The small scatterer indicated by the orange circles in the figures is associated with a dipping metal pipe oriented 45 degrees relative to the profile line direction.

There are very noticeable differences between Figs 3 and 5 and between Figs. 7 and 10 associated with the parallel and perpendicular pipes buried in sand. Some amplitude and phase difference would be expected associated with the different polarizations. But there are several reflection events apparent in Fig. 10, for example, such as the reflection from the metal pipe in the bottom left corner, that are weakly present in Fig. 7.

One explanation for this would be a moisture difference in the sand. The arrival time difference between the same targets in the two different datasets increased with depth and ranged from 0.5 to over 2 ns. Some repeat perpendicular polarization profile lines obtained the same day as the parallel polarization data were compared to the perpendicular polarization data obtained 11 days prior. The 0.5 – 2 ns arrival time difference was also observed in these files obtained over the same pit locations. A review of the weather records indicates that the early portion of August was particularly wet, with two weather stations within 10 km of the test pit reporting 1.0 and 1.6 cm 9 days prior to collecting the August 25th dataset. The rainfall, coupled with known cracks in the pavement at the pit boundaries due to settling, provide a compelling explanation for the presence and infiltration of water through the sand during collection interval.

V. Discussion

The full-resolution technique applied with the polarization direction parallel or perpendicular to the data collection direction yielded images that permitted detection of all the targets. Acquiring a 0.05m by 0.05m (x,y) grid, although time consuming, meant that in-line pipes could be resolved without needing an extra perpendicular 3-D survey, making acquisition times similar, and post-processing less complicated. The 2.5D migration approximation also makes post processing faster and less complicated than a 3-D migration while still providing the resolution necessary to differentiate closely spaced utilities.

The fact that all of the targets were detectable with both data collection polarizations was not surprising after a comparison of the reflection amplitudes versus polarization revealed a maximum difference of approximately 6 dB and the minimum reflection amplitude was much greater than the signal noise floor. For other more challenging scenarios in conductive clays, the 6 dB difference in amplitude associated with polarization may become significant. In such cases, the over-sampled depth resolution that was collected (instead of 0.05m) may be useful both to improve signal to noise and to give the greater slice precision needed for resolving faint differences in the data.

The increased data quality and density of full-resolution GPR brings compelling benefits in several standard applications. For example it would improve the ability to distinguish pipes in crowded utility trenches. Time lapsed assessment of pipe condition can be made more accurate, since increased resolution makes subtle changes in soil

moisture more detectable. Leak detection or plume monitoring over time could be made more accurate as well.

Furthermore, full-resolution imaging makes automatic pipe detection algorithms more robust, saving hours of time on data interpretation. And volume rendering capabilities are more accurate, making data analysis and inferences more quantitative and reliable.

VI. Conclusion

Full-resolution GPR data collection provides superior imaging compared to traditional 3D GPR. The full-resolution images make it easier to locate and differentiate targets and to delineate disturbed areas of soil. Where possible, most GPR applications for soil and utility mapping and monitoring would benefit directly from full-resolution data collection.

In fact of the three reasons against performing full-resolution surveys, 1) time consuming acquisition, 2) consistent data registration and 3) the expensive post-processing time, (2) remains the most difficult to achieve. This survey on a level paved surface, using a heavy "straight edge" is impractical in most situations. And although for most general purpose surveys the time and material costs required to produce such datasets are prohibitive, it is anticipated that incremental advances in GPR technology and positioning systems will eventually allow these surveys to be done more easily and hence unlock the potential of full-resolution imaging.

VII. Acknowledgment

The authors appreciate the assistance of Mike Jeffords and Doug Kenny during data collection.

References

[1] M. Grasmueck, R. Weger, and H. Horstmeyer, "Full-Resolution 3D GPR Imaging," *Geophysics*, vol. 70, pp. K12-K19, Jan. 2005.

[2] M. Grasmueck and D. Viggiano, "3D/4D GPR Toolbox and Data Acquisition Strategy for High-Resolution Imaging of Field Sites," in *Proc. 11th International Conference on Ground Penetrating Radar (GPR 2006)*, Columbus, OH , June 19-22, 2006, 6p.

[3] A. Novo, M. Grasmueck,D. Viggiano, H. Lorenzo, "3D GPR in Archeology: What can be gained from dense Data Acquisition and Processing?" in *Proc. 12th International Conference on Ground Penetrating Radar (GPR 2008)*, Birmingham, UK , June 16-19, 2008, 5p.

[4] Gardner, G.H.F., McDonald, J.A., Watson, T.H., and Kotcher, J.S., 1978, An innovative 3-D marine seismic survey: Presented at the 40th Ann.Assoc. Explor. Geopys. Mtg.

[5] Yilmaz, O., 1987, Seismic Data Processing. Society of Exploration of Geophysicists, P. 403.